Artificial Fish Schools: Collective Effects of School Size, Body Size, and Body Form

Hanspeter Kunz[1]
Charlotte K. Hemelrijk[1,2]
[1]Artificial Intelligence Laboratory
Department of Information Technology
University of Zürich
Andreasstrasse 15
8050 Zürich
Switzerland

[2]Anthropological Institute and Museum
University of Zürich
hkunz@ifi.unizh.ch
hemelrij@ifi.unizh.ch

Abstract Individual-based models of schooling in fish have demonstrated that, via processes of self-organization, artificial fish may school in the absence of a leader or external stimuli, using local information only. We study for the first time how body size and body form of artificial fish affect school formation in such a model. For a variety of group sizes we describe how school characteristics (i.e., group form, spread, density, polarization, turning rate, and speed) depend on body characteristics. Furthermore, we demonstrate that the nearest neighbor distance and turning rate of individuals are different for different regions in the group, although the agents are completely identical. Our approach shows the significance of both self-organization and embodiment in modeling of schools of artificial fish and, probably, in structuring schools of real fish.

Keywords
Schooling, embodiment, collective behavior, emergence, group size, body size and form

1 Introduction

In studies of artificial life and artificial intelligence the effects of self-organization and embodiment are important topics. In the present article we investigate both aspects in the context of simulated artificial fish schools. We analyze how self-organization may lead to emergent behavioral phenomena [5] at different group sizes and how this process may be affected by characteristics of the body and may influence collective behavior [18, 19]. Several individual-based models of schooling in fish [1, 6, 9, 11, 13, 20, 22, 24] have revealed that artificial fish, which use local information only (like flocking birds; see [21]) may school in the absence of a leader and external stimuli. Further, some of them have shown certain collective effects of school size, but the origin of these effects has not been explained. By studying both group size and body characteristics (forms and sizes), we hope to obtain insight into the processes that lead to these collective effects.

Our model is inspired by those due to Huth and Wissel [10, 11], Reuter and Breckling [20], and Niwa [13]. In these models schooling is a consequence of the tendency of fish to avoid others that are close, to align their body to those at intermediate distances, and to move towards others that are far away. Shaw [23] had already suggested such distance dependent mechanisms and distinguished between polarized, coordinated "schools" and non-polarized, non-coordinated "shoals." Here, we investigate the former only.

In earlier models of fish schools, fish are represented as points and their regions of repulsion, alignment, and attraction are concentric and circular. This does not reflect the form and size of the agent's body or its sensory capabilities. Modeling the agent's

body with its sensory characteristics may alter the way the agent is perceived by others as well as the way it perceives its neighbors. Therefore, we compare the schooling behavior of artificial fish represented as lines with that of fish represented as points. Furthermore, not only vision, but also the lateral line is used in schooling [2, 17]. Lateral lines consist of a series of hydrodynamic sensors along both sides of the body [2]. They detect stimuli (i.e., changes in water flow) close to the body only. We reflect this in the model by making the shape of the repulsion and aligning areas elliptical in form. Therefore, we compare the collective behavior of artificial fish with circular areas of alignment and repulsion with that of fish with oval-shaped ones. Further, we investigate artificial fish of two different body sizes. Here, we follow the findings by Olst and Hunter [14] that larger fish have larger repulsion areas, but the increase with body size is less than proportional.

In sum, we compare the collective behavior of artificial fish of different body sizes and forms in increasing detail for various group sizes. Apart from traditional statistical measures, we also use measures developed by ourselves (viz., a measure of spatial homogeneity, a measure of the relative location of the center of gravity within the school, and a measure of group form). We will explain how self-organization and embodiment influences collective patterns of artificial schools of different sizes. Subsequently, we will indicate how these results may guide studies of real fish.

2 Methods

Our model contains aspects of several models by others. As in the model by Huth and Wissel [10], fish react to each other by repulsion, by alignment, and by attraction. In agreement with Reuter and Breckling [20] and Niwa [13], these behavioral tendencies are weighted according to distance, and thus result in graded transitions between the different motivations.

Fish schools have been modeled in 2D as well as in 3D. On comparing a particular 2D model [10] with a 3D one [12], no additional phenomena were observed in the 3D model. Therefore we decided to implement our model, SchoolingWorld, in 2D.

2.1 The Model

The model consists of a world that is continuous (not a grid), in which artificial fish can move. The environment is homogeneous (without structure). Time proceeds in discrete steps Δt. At each time step all artificial fish are activated sequentially in random order. However, for parallel activation (where all agents are activated simultaneously) the same results are obtained. The model was implemented in C. Octave and Gnuplot were used for data analysis.

2.1.1 Position, Speed, and Heading

At the beginning of the simulation, a certain number of artificial fish are put randomly in a starting area of 2.5 by 2.5 m and are given a random orientation, which was chosen between 0 and 90° in order to result in a single school. The initial speed of the agents was set to v_{avg} (see Table 1).

At time t agent i is located at position $\mathbf{x}_i^t$ and moves with a velocity $\mathbf{v}_i^t$ during one simulation step Δt:

$$\mathbf{x}_i^t = \mathbf{x}_i^{t-\Delta t} + \mathbf{v}_i^t \Delta t \tag{1}$$

Table 1. Simulation parameters.

Parameter	Symbol and value
Simulation time step	$\Delta t = 0.2$ s
Average and standard deviation of agent speed	$v_{\text{avg}} = 0.3$ m/s, $v_{\text{sd}} = 0.03$ m/s
Standard deviation of agent heading	$\alpha_{\text{sd}} = \frac{\pi}{72}$ rad $\cong 2.5^\circ$
Default rate of rotation of the agents	$\omega^{\text{def}} = \pi$ rad/s
Body length	Point agents: $b = 0.0$ m
	Large agents (line, elliptic): $b = 0.2$ m
	Small agents (line, elliptic): $b = 0.1$ m
Scaling factor for repulsion	Large agents: $a_r = 2.0$
	Small agents: $a_r = 1.0$
Scaling factor for alignment	$a_p = 1.0$
Scaling factor for attraction	$a_a = 1.0$
Repulsion range	Large: $r_r = 0.6$ m
	Small: $r_r = 0.3$ m
Alignment range	Large: $r_p = 2.0$ m
	Small: $r_p = 1.0$ m
Attraction range (visual range)	$r_a = 5.0$ m
Eccentricity of repulsion and alignment regions	Point and line agents: $e = 1.0$
	Large elliptical agents: $e = 4.0$
	Small elliptical agents: $e = 2.0$

The velocity $\mathbf{v}_i^t$ is determined by the agent heading α_i^t (orientation of the vector $\mathbf{v}_i^t$) and by the speed v_i^t (length of the vector $\mathbf{v}_i^t$) as follows:

$$\mathbf{v}_i^t = \begin{pmatrix} v_i^t \cos \alpha_i^t \\ v_i^t \sin \alpha_i^t \end{pmatrix} \tag{2}$$

Similarly to certain models of fish schools [1, 6, 10, 12], the speed v_i^t of agents does not depend on that of other agents, but is an independent stochastic variable. It is drawn from a Gaussian probability distribution $P(v_{\text{avg}}, v_{\text{sd}})$ each time step. The stochasticity is chosen to reflect unspecified variation in speed.

The heading α_i^t of agent i is determined by

$$\alpha_i^t = P(\underbrace{\alpha_i^{t-\Delta t} + \omega_i^t \Delta t}_{\alpha_{i,\text{avg}}^t}, \alpha_{\text{sd}}) \tag{3}$$

where $\alpha_i^{t-\Delta t}$ is the agent's heading in the previous simulation step and ω_i^t is its rate of rotation, which depends on the interaction with the other agents (see Section 2.1.2). α_i^t is again drawn from a Gaussian distribution $P(\alpha_{i,\text{avg}}^t, \alpha_{\text{sd}})$.

2.1.2 Repulsion, Attraction, and Aligning

The artificial fish have three types of behavioral responses, namely repulsion (short distances), attraction (intermediate distance), and alignment (greater distances) [3, 25]. This has often been modeled by splitting the region surrounding the agent into behavioral zones with definite boundaries (see, e.g., [10]); therefore an agent triggers exactly one type of behavioral response in a neighbor. An alternative approach, which is

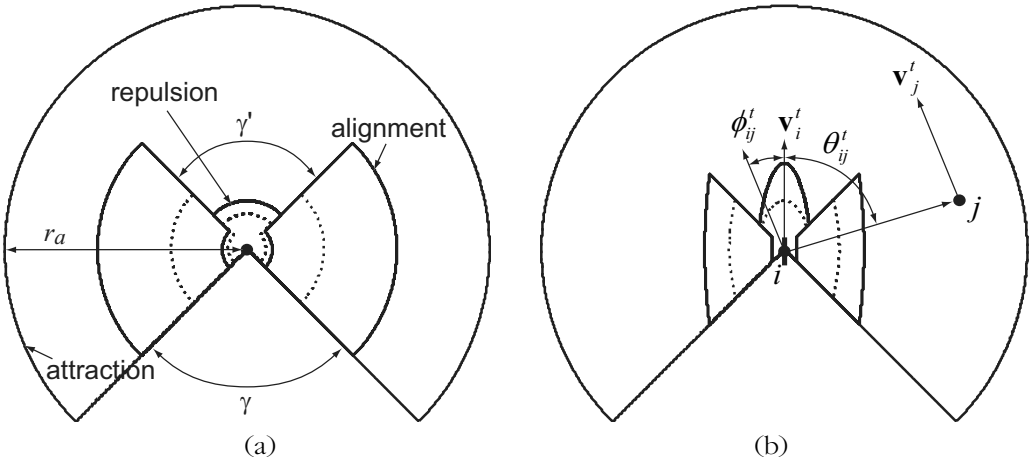

Figure 1. Schematic representation of the different behavioral regions of an agent. The agent is located at the center. The outermost circle shows its visual range r_a, which can be divided into three functional areas, namely attraction, alignment, and repulsion. (a) Point agents (dotted lines indicate the attraction and repulsion regions of small agents; solid lines, of large ones). Note that line agents are the same except for a line representing their body instead of a point. (b) Elliptical agents; body size is indicated by the small line segment at the center. See text for further information.

adopted here, is the use of continuously varying distance dependent weight factors to determine the effectiveness of repulsion, alignment, and attraction behaviors (see, e.g., [13, 20]). Thus, an agent triggers all three types of behavioral responses in a neighbor, although with different effectiveness.

In their experimental studies of real fish, Partridge and Pitcher [17] have shown that the three behavioral responses are mediated by different sensory systems (lateral lines and visual system) to a different extent. Cutting the lateral lines makes it difficult for fish to align their swimming direction to others and to keep others at a minimal distance, whereas blindfolding fish impairs social attraction.

We assume that attraction, mediated mainly by vision, operates in the whole visual range around the agent apart from a blind area in the back with an angle of $\gamma = 60^\circ$ (Figure 1a). For alignment, for which the lateral line is considered to be the most important sensory system, there is an additional blind area at the agent's front (Figure 1a, $\gamma' = 60^\circ$). Thus the lateral line is most effective at the sides, and it operates at intermediate distances. Repulsion, mediated by both lateral line and vision, operates over the whole visual range (Figure 1a).

Repulsion implies that an agent i turns away from a close-by agent j with an rate of rotation (angular speed) of

$$\omega_r = \begin{cases} -\omega^{\text{def}} & \text{if } \theta_{ij}^t > 0 \quad \text{(avoid agent to the left)} \\ +\omega^{\text{def}} & \text{otherwise} \quad \text{(avoid agent to the right)} \end{cases} \tag{4}$$

where $\theta_{ij}^t = \angle(\mathbf{v}_i^t, \mathbf{x}_j^t - \mathbf{x}_i^t)$ (see Figure 1b) and ω^{def} is the default rate of rotation of the agents (Table 1), reflecting their movement capabilities. Attraction implies that an agent i turns towards an agent j with a rate of rotation of

$$\omega_a = \omega^{\text{def}} \theta_{ij}^t \tag{5}$$

Note that, in contrast to repulsion, the rate of rotation ω_a caused by attraction is proportional to θ_{ij}^t. Aligning implies that agent i matches its orientation to that of agent j by turning with a rate of rotation

$$\omega_p = \omega^{\text{def}} \phi_{ij}^t \tag{6}$$

where $\phi_{ij}^t = \angle(\mathbf{v}_j^t, \mathbf{v}_i^t)$ is the angle between the orientations of the two agents (Figure 1b). The actual behavioral reaction depends on the weights of repulsion (w_r), attraction (w_a), and alignment (w_p), depending on the distance to the other agent:

$$d_{ij}^t = \|\mathbf{x}_j^t - \mathbf{x}_i^t\| \tag{7}$$

$$w_r(d) = \min\left(\frac{0.05 a_r}{d^3}, 10\right) \tag{8}$$

$$w_a(d) = 0.2 a_a \exp\left[-\left(\frac{d - \frac{1}{2}(r_a + r_p)}{r_a - r_p}\right)^2\right] \tag{9}$$

$$w_p(d) = a_p \exp\left[-\left(\frac{d - \frac{1}{2}(r_p + r_r)}{r_p - r_r}\right)^2\right] \tag{10}$$

(see Figure 2 and Table 1 for the parameters). The combined behavioral reaction (i.e., rate of rotation) of agent i due to the interaction with a single agent j is calculated as a weighted sum

$$\omega_{ij}^t = w_r(d_{ij}^t)\omega_r + w_a(d_{ij}^t)\omega_a + w_p(d_{ij}^t)\omega_p \tag{11}$$

The weight factors cause the behavioral reaction to depend continuously on the distance. Therefore, there is no discrete behavior switching. Nevertheless, for convenience, we label three behavioral regions after the largest of the three weighting factors (Figure 2).

When agent i perceives more than one other agent j (by either vision or the lateral line), its behavioral response (rate of rotation) is calculated as the average of the responses it would display when considering each neighbor independently, that is, the average of the rate of rotation caused by each of the agents j separately:

$$\omega_i^t = \frac{1}{N_i} \sum_j \omega_{ij}^t \tag{12}$$

Here N_i denotes the number of agents perceived by agent i. Note that ω_{ij}^t describes the behavioral reaction (rate of rotation) of agent i in response to the presence of agent j (not to be confused with the rate of rotation ω_j^t of agent j).

2.1.3 Body Size and Form

Three aspects of the agents were varied to reflect body characteristics. First, we represent the agent's body by a line segment of variable length b instead of a point (Table 1). This does not change the agent's behavior directly, but it alters the way the agent is perceived by others as follows. Instead of using the distance between the agents' centers, d_{ij}^t, to measure the distance between two agents, the distance between agent i's center and the nearest point of agent j, denoted as D_{ij}^t (Figure 3) was used in Equation 11. Note that D_{ij}^t and d_{ij}^t differ depending on the body size b (Figure 3).

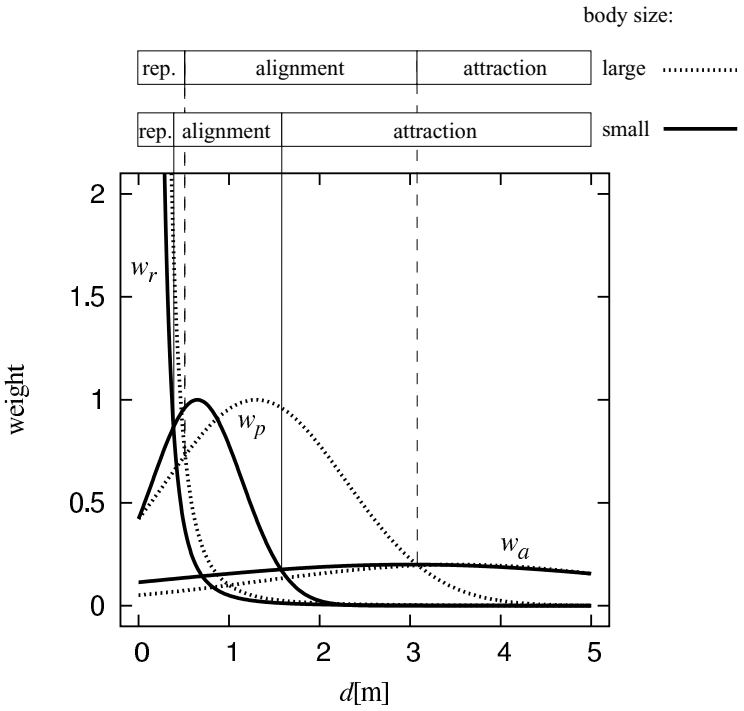

Figure 2. Plot of the weight factors $w_r(d)$, $w_a(d)$, and $w_p(d)$ for small agents (solid lines) and large ones (dotted lines). d denotes the distance to the neighbor. Regions are classified into repulsion (rep.), alignment, and attraction according to the largest of the three weight factors (top of figure).

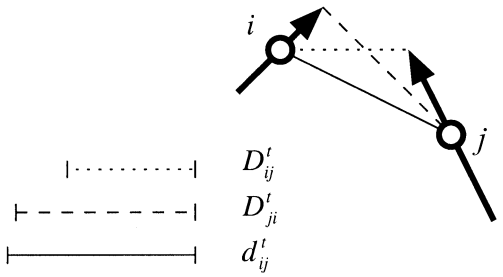

Figure 3. Measures of distance between agents. d_{ij}^t denotes the Euclidean distance between the centers of the two agents. D_{ij}^t and D_{ji}^t denote alternative approaches to calculating agent distance, depending on both body size and form (see text for details).

Second, as regards body size we follow the findings by Olst and Hunter [14] that larger fish maintain larger inter-individual distances, but they are closer than would be expected if inter-individual distance were proportional to the body size. This is modeled by increasing the sizes of the repulsion and alignment regions (by changing the values of a_r, r_r, and r_p; see Figures 1 and 2, Table 1, and Equations 10 and 11). The range of attraction (mediated by vision) was kept identical.

Third, body form is modeled by including sensory characteristics of the lateral line, thereby changing the agent's perception of its neighbors. We assume that the perceptual field of the lateral line follows the body form; therefore the repulsion and alignment regions are elliptical rather than circular (Figure 1b). This is achieved by redefining the

agent distance d_{ij}^t used in Equation 11. Consider an agent j at position (u_j, z_j) relative to a coordinate system embedded in agent i, in such a way that the u axis points in the heading direction α_i^t of agent i. For elliptical agents the distance between agent i and j is defined as

$$e_{ij}^t = \sqrt{\frac{1}{e}u^2 + ez^2} \tag{13}$$

where e is the eccentricity (Table 1). Therefore, if agent j is located directly in front of agent i ($z = 0$), then e_{ij}^t is smaller than d_{ij}^t, and if agent j is at the side of agent i ($u = 0$), then e_{ij}^t is larger than d_{ij}^t. Consequently, agents will avoid those neighbors that are ahead of them sooner (at a greater distance) than those that are at their side (in accordance with the elliptical form of the repulsion region; see Figure 1b). The same applies for the alignment region.

Body form is modeled as follows in three levels of increasing detail (see Table 1):

1. *Point agents:* Agents are modeled as points; body size is only reflected in the size of the regions of repulsion and alignment. Agents of larger size have larger regions of repulsion and alignment, but their range of attraction (their vision) is the same for all (see Figure 1a; solid lines: regions of large agents, dotted lines: those of small agents).
2. *Line agents:* Agents are represented as lines. Larger body size is reflected in longer lines and larger regions of repulsion and alignment (Figure 1a).
3. *Elliptical agents:* Agents are represented as lines. The regions of repulsion and of alignment are elliptical and are larger for large agents than for small ones. The region of attraction is circular and independent of body size (Figure 1b).

Note that we have included the line agents merely as a kind of control, to study the effects of the representation of the agent's body as a line.

2.2 Experiments

For agents with body length b of 0.2 m (large) and 0.1 m (small) and for all three types of body form, we have studied eight population sizes of 3, 4, 6, 10, 25, 50, 75, and 100 identical agents. Every simulation was repeated 25 times from random starting locations. For parameters see Table 1.

2.3 Measures

At each simulation step the following statistics have been calculated.

To measure the group spread, we use the average distance of all agents to the center of the group, the so-called *average center distance* c^t:

$$c^t = \frac{1}{N}\sum_i \|\mathbf{X}^t - \mathbf{x}_i^t\|, \qquad \mathbf{X}^t = \frac{1}{N}\sum_i \mathbf{x}_i^t$$

where $\mathbf{X}^t$ denotes the center of gravity of the school. A similar measure, *expanse* (i.e., average squared distance to the center of the group) was used by Huth and Wissel [10].

To measure group density we use the average *nearest neighbor distance* n_1^t (see for instance [10]). We quantify the uniformity of the spatial distribution of agents, called *homogeneity*, by the average distance to the nearest neighbor divided by the distance to the second nearest neighbor (n_1^t / n_2^t). High homogeneity of spatial distances among

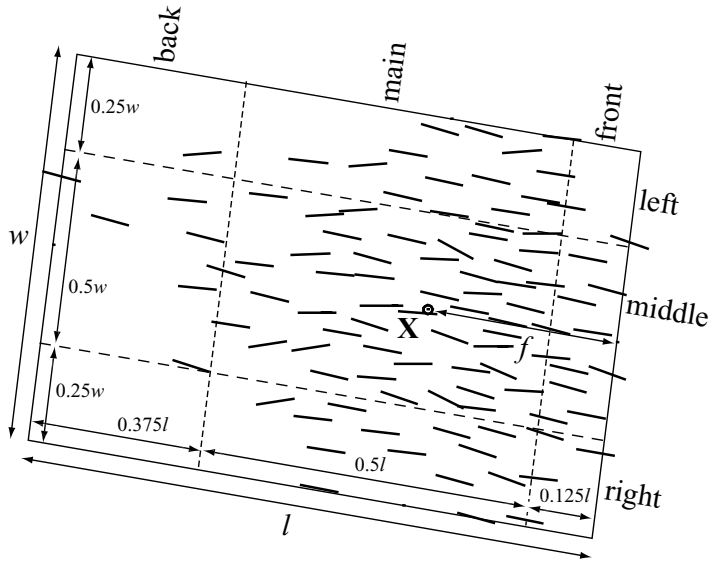

Figure 4. The box method for obtaining measures of group width w, length l, and front length f. Dashed lines indicate the different regions of measurement.

agents is reflected by values close to one, whereas high irregularity (low homogeneity) of agent distribution results in lower values.

To quantify the coordination of the heading directions of the agents, we calculate the square root of the mean quadratic angular deviation of each fish from the average heading α^t_{avg} of the group:

$$p^t = \sqrt{\frac{1}{N}\sum_i (\alpha^t_{\text{avg}} - \alpha^t_i)^2}, \qquad \alpha^t_{\text{avg}} = \frac{1}{N}\sum_i \alpha^t_{ij}$$

p^t is usually referred to as *polarization* [10], but we call it *confusion*, since higher values indicate greater disorder. Note that by "homogeneity" we mean spatial uniformity of the locations of the agents, whereas confusion and polarization measure the coordination (unidirectionality) of the headings the agents.

Further, the *group speed* v^t_g is defined as speed of the center of gravity $\mathbf{X}^t$ of the group; the *group turning rate* T^t_g, as the (absolute) rate of change of direction of the group.

To measure school form, we enclose the whole school in the smallest rectangle oriented parallel to the direction of movement of the group (Figure 4) and characterize group form by the *length* l^t, the *width* w^t, and their quotient q^t (width divided by length). To indicate the relative place g^t of the center of gravity $\mathbf{X}^t$ in the school, we use the distance of the center of gravity to the front (called the front length f^t) divided by total length (l^t).

In order to detect spatial variations, we partition the group in two ways: into the left, middle, and right parts, and into the front, main, and back parts (Figure 4). In each of these parts we calculate separately the average *agent turning rate* [i.e., the (absolute) rate of change of the agent's heading direction] and average nearest neighbor distance. We denote the average agent turning rate by T^t_f and the average nearest neighbor

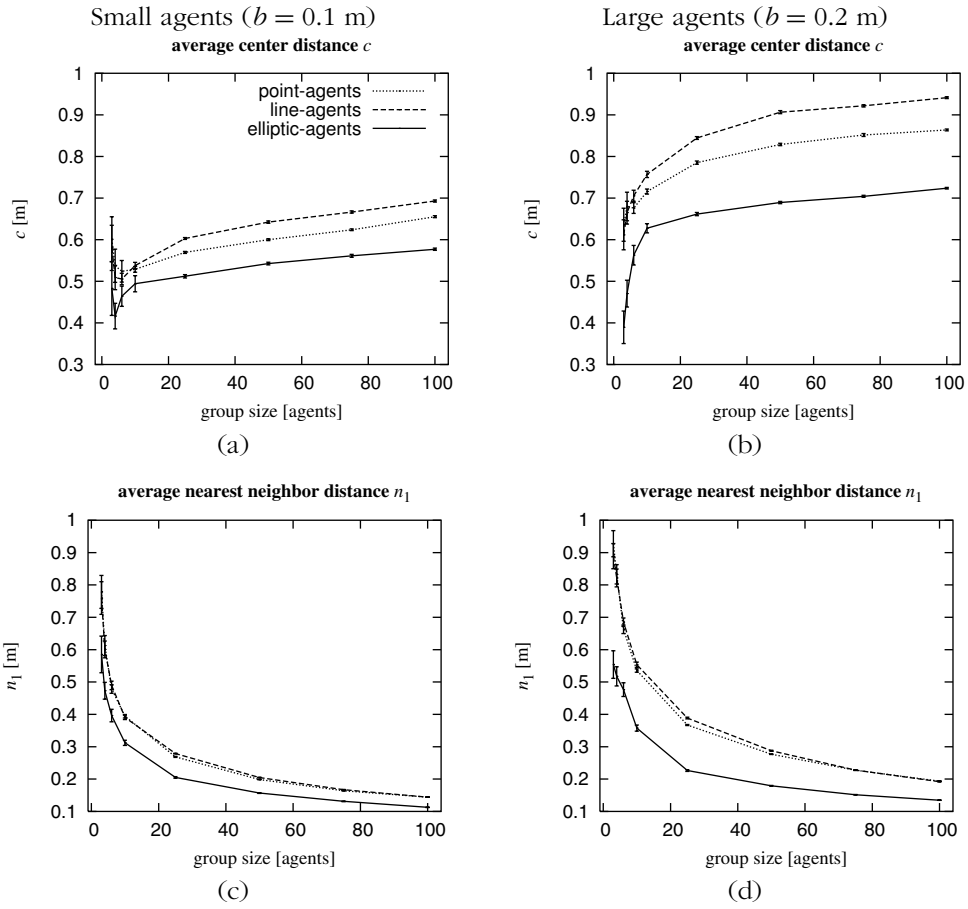

Figure 5. Distance measures and their standard errors for different sizes of groups of agents that are small (a, c) and large (b, d).

distance by n_f^l. The subscripts denote the section (f: front; n: main; b: back; l: left; m: middle; r: right).

For each simulation the measures were averaged over time steps 2000–3000 (thus omitting the transient period). Averages and their standard errors over 25 runs are plotted in the figures in Section 3. We discuss only the results that differ significantly as judged by the small size of the standard errors. Further, we only evaluate runs where the agents aggregate in a single school. This was the case in 98.9% of the simulations.

3 Results

3.1 General Effects of Group Size

As a direct consequence of the larger number of individuals in larger schools, the average distance to the center increases with school size (Figure 5a,b), because a larger group covers a larger spatial area. Nevertheless the nearest neighbor distance decreases (Figure 5c,d) with increasing group size, due to the increased attraction among the larger number of group members, which leads to a denser packing of agents.

Because agents do not align directly with more remote group members in a larger group, the confusion (mean angular deviation) increases (Figure 6a,b), and this leads

to a lower speed of the group[1] (Figure 6c,d). The turning rate of larger groups is lower (Figure 6e; data for large agents are similar, but not shown). This is a consequence of the greater number of individuals that have to coordinate in order for the whole group to turn.

The center of gravity is significantly found in the front half of the school: The distance from the center of gravity to the front divided by the distance to the back was always smaller than 0.9 (for an example see Figure 4). There are two causes for this. First, due to the constant speed, agents cannot catch up once they lag behind. Second, agents near the front have few individuals ahead of them. Therefore they have a smaller tendency to move straight forward, but they may turn either left or right, whenever they perceive more neighbors on the other side. Consequently, their turning rate is higher than that of agents in the main and the back region, which are also attracted to others ahead (Figure 7b,d). Due to their increased turning rate, the front agents slow down slightly, which leads to crowding at the front. Also, the turning rate is lower at the sides than in the middle part of the school (Figure 7f), especially for the elliptical agents.

The finding that the center of gravity is in the front half of the school is also reflected in the relative nearest neighbor distances in different parts of the group (Figure 7a,c). The nearest neighbor distance is lowest in the main part and highest in the back, whereas it is intermediate at the front. It is also lower in the middle part than in the sides (Figure 7e).

Increasing group size leads to an increase in both the width and length of the group (Figure 8a–d). The width of the group increases slower at larger group sizes (Figure 8a,b), whereas the length of the group grows almost linearly with group size (Figure 8c,d). This may be due to the fact that in wide groups there is a strong attraction to the center among peripheral agents. This results in a strong inward movement of the agents located at the sides, whereas there is no similar mechanism for agents in the front or at the back of the school, because of their constant speed. Therefore, large groups are longer than they are wide (Figure 8a,b,c,d).

3.2 Effects of Body Size and Form

Larger agents are usually significantly further apart than smaller ones (as measured by average distance to the center and nearest neighbor distance; note the small values of the standard error in Figure 5a–d). This is due to their larger body size and repulsion area. For a similar reason, when comparing different agent types of the same body size, line agents are significantly further apart than point agents. For point and line agents, the nearest neighbor distance is approximately the same, whereas the average center distance is larger for line agents. This arises because line agents swim at larger distances behind each other, whereas swimming side by side they stay as close as point agents do. Elliptical agents swim significantly closer together side by side, due to their narrow and long (elliptical) repulsion region (Figure 1b).

The uniformity of distances (i.e., homogeneity) among group members (measured in terms of the ratio of the distances to the first and second nearest neighbor) is weaker the more asymmetric the body form is. Thus, homogeneity decreases from point, to line, to elliptical agents (Figure 6f; similar data for small agents are not shown).

Between groups of large and small agents, the group turning rate appears to be similar, but the confusion and consequently the group speed differ in a different way among groups of line and point agents on the one hand and elliptical agents on the other. Groups of large line (and point) agents show less variation in heading direction,

1 This is explained geometrically. The velocity component in the direction of the group heading of an agent with an angular deviation $\Delta\alpha$ is $v_{avg} \cos \Delta\alpha$. Consequently for the group speed we have $v_g \approx v_{avg} \cos p$, as p is a measure of the mean angular deviation.

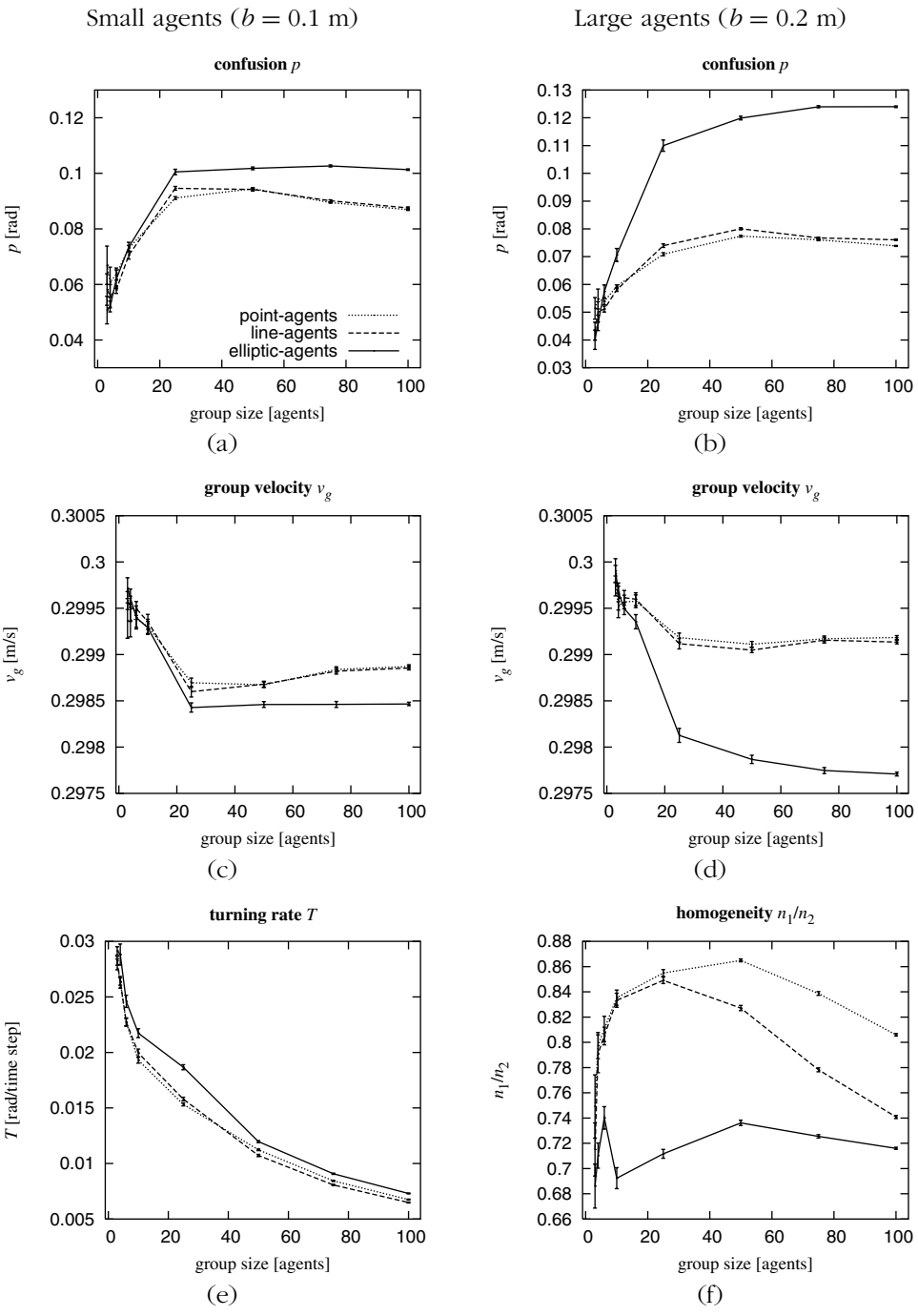

Figure 6. Mean values and standard errors of confusion (a, b), group speed (c, d), group turning rate (e), and homogeneity of distances (f) of groups of large agents (right panels) and of small ones (left panels) for different group sizes.

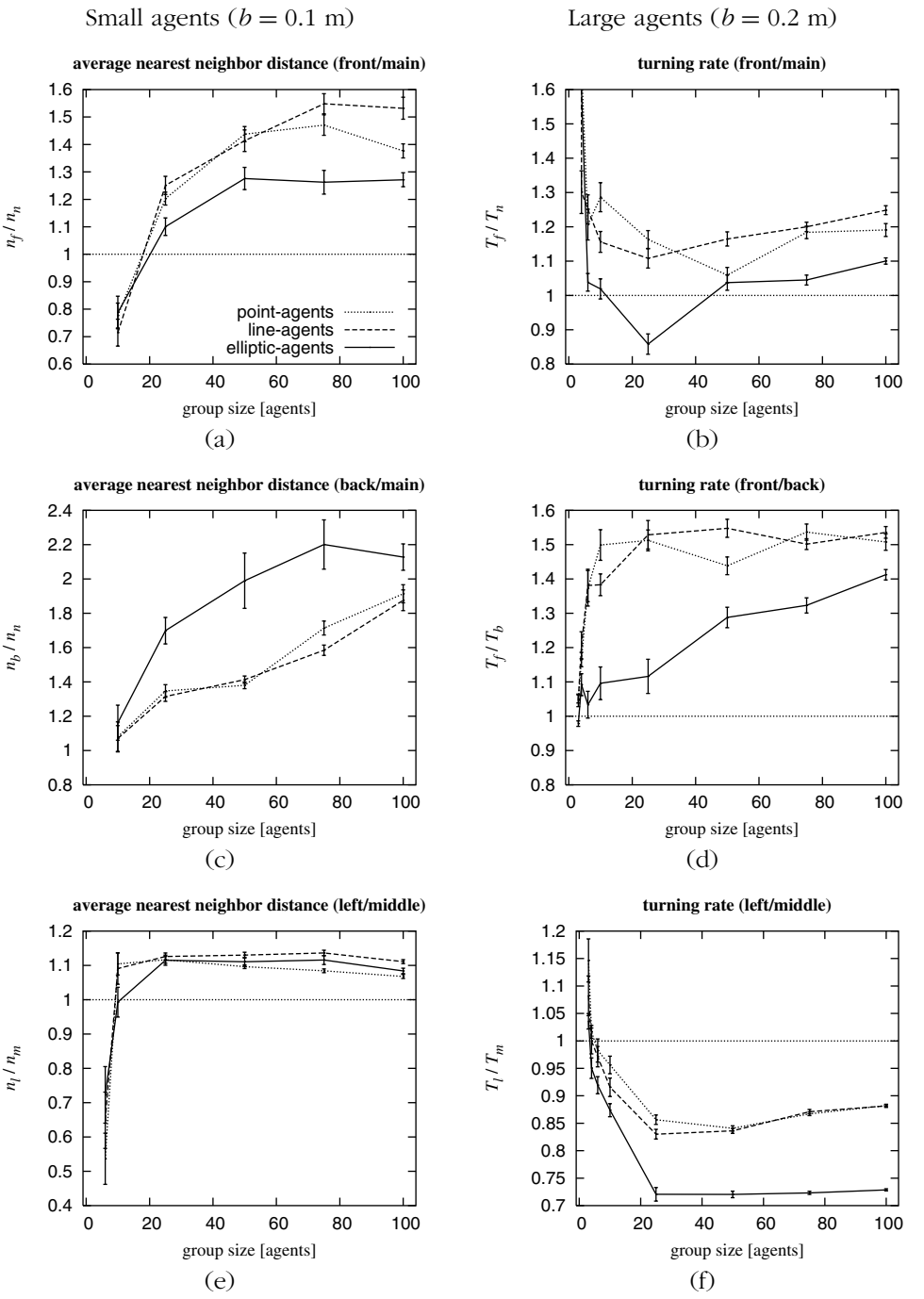

Figure 7. Left panels: Mean and standard error of ratio of average nearest neighbor distances in different parts of groups of several group sizes consisting of small agents (the results for large agents are qualitatively similar). Right panels: Mean and standard error of ratio of average agent turning rates in different parts of the group for several group sizes of large agents (the results for small agents are qualitatively similar).

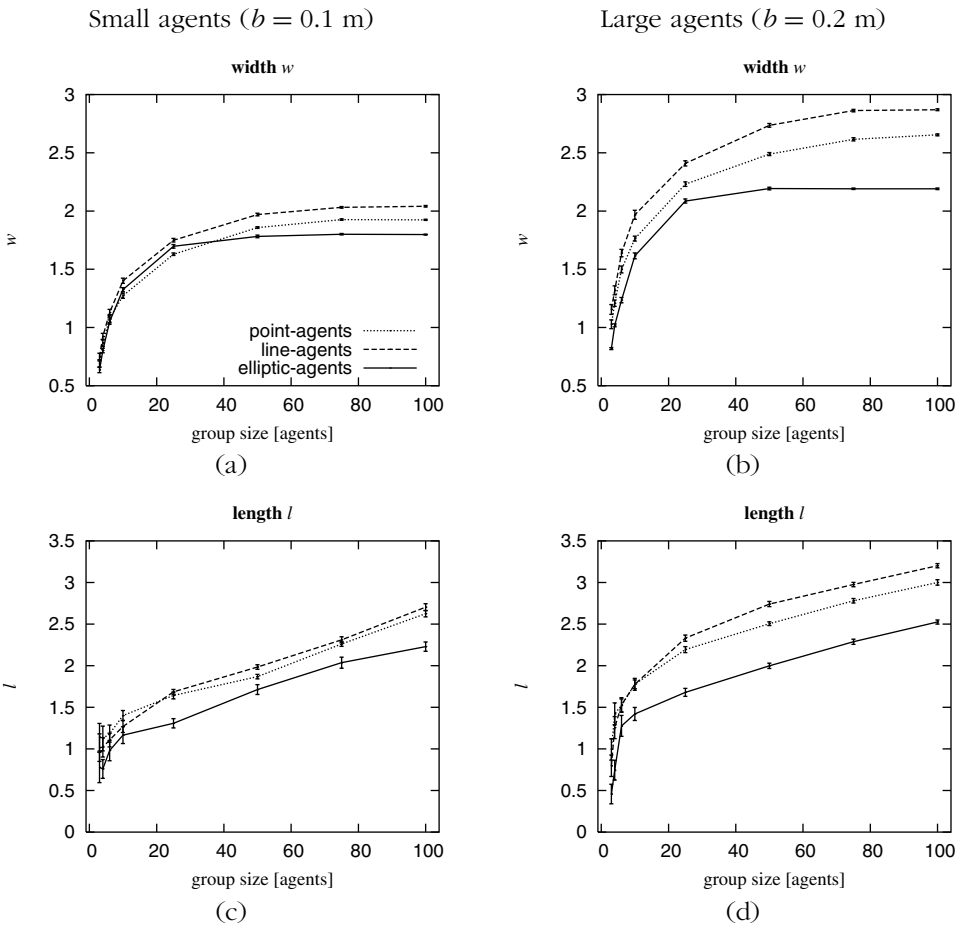

Figure 8. Average and standard error of group width and length for several group sizes of either small agents (left panels) or large ones (right panels). For definitions of width and length see Figure 4.

and therefore higher speed, than groups of small agents. For elliptical agents, however, the reverse holds (Figure 6a–d). Heading directions of point and line agents that are large are more coordinated than those of agents that are small, due to the greater alignment area of larger agents (Figure 1a). In contrast, among elliptical agents the elliptical form of the repulsion area causes frequent turning. Because the repulsion area is long, after turning away from certain group members, the individual soon finds others in its repulsion region, and this provokes another repulsion reaction (Figure 9). This *repeated-repulsion effect* is greater for large elliptical agents than for small ones, because the form of the repulsion region for large ones is more asymmetric (Figure 1b). In sum, groups of elliptical agents (of both sizes) show greater confusion of heading directions than groups of point and line agents, due to the combined effects of repeated repulsion and the smaller size of their alignment region (Figure 1a,b).

As regards group form, line agents form the widest and longest groups, groups of point agents are intermediate and those of elliptical agents are smallest (Figure 8a–d). The difference between line and point agents is due to the smaller bodies of the latter. Groups of elliptical agents, in turn, are smaller due to their narrower repulsion area. Groups of large agents appear to be wider (Figure 8a,b) and more circular (data not shown) than those of small agents. This is possibly because the attraction at the sides

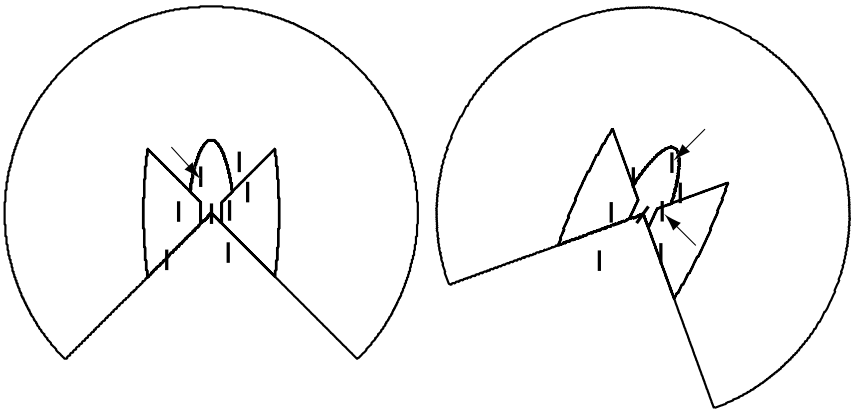

Figure 9. Effect of elliptical repulsion regions on agent behavior (repeated repulsion effect): An agent (center) avoids a close-by agent (indicated by an arrow, left panel) by turning away (right panel). Because of the elliptical form of the repulsion region, other neighboring agents may be found in the repulsion region after the turn (indicated by arrows in the right panel), which will induce another avoidance movement in the next time step.

of the agents is weaker as a consequence of the greater alignment area. For all types, we find elongated schools (data not shown), at least at larger group sizes ($N > 50$).

4 Discussion

Our model, SchoolingWorld, shows several emergent phenomena: the number of agents in a group influences the group's form, density, confusion, turning rate, and group speed. Further, although all agents are completely identical, the agent density varies depending on the location in the school (e.g., front or back). An elliptical body form leads to a more confused school and therefore to reduced group movement.

As regards the effects of group size, SchoolingWorld shows that larger groups have a higher agent density, are more confused, and have a lower group speed. A larger expanse (which is similar to the average center distance) of larger groups, and, simultaneously, a decreased average nearest neighbor distance for larger groups has also been found in earlier models [9, 20], but no explanation has been given for this phenomenon. Here, we explain such closer proximity to the average nearest neighbor (huddling together) by the stronger mutual attraction in larger groups due to the larger number of neighbors. Further, the increase in confusion (average deviation of the headings of the agents from the group average) in larger groups is in line with the findings of Reuter and Breckling [20]. It arises because in larger groups only a part of the agents directly align with each other (because of the larger agent distances). For geometrical reasons, higher confusion lowers group speed. The turning rate of larger groups in SchoolingWorld is slower due to the smaller impact of the behavior of a single agent on the group and because there are more agents present to align with. This result contrasts with some of the results by Romey [22]. Whereas he found that the speed of groups decreased in larger groups, simultaneously (in contrast to our results) the group turning rate increased in larger (cohesive) groups. This difference may be attributed to the absence of alignment in his model. Therefore, turning movements, which occur frequently in dense (large) groups because of repulsion, are not damped by alignment and thus may more easily lead to a change of direction of the whole group.

How do these effects of group size in SchoolingWorld relate to findings in real animals? A smaller inter-individual distance in larger schools has been found in many fish studies (minnows [15]; cod and saithe [16]). This makes it interesting to investigate

confusion and group speed in relation to group size also. Such data would reveal whether our model captures the essentials of fish schooling. If so, we may expect larger groups to fission more easily as a consequence of the increased confusion.

Although the agents are completely identical, they behave differently in different parts of the group. The average turning rate of agents is highest at the front. This arises because agents at the front have no group members ahead of them and thus are attracted only to the partners at their sides. This causes the agents at the front to slow down and thus leads to a jam near the front. Thus, in our model agents are distributed unevenly in the school. The density is higher in the center and at the front, and lowest at the back, and therefore the center of gravity is located in the front half of the school. Further, for larger group sizes, schools are usually longer than they are wide, and this asymmetry increases with the number of agents. In our model these properties are emergent from the combination of attraction and aligning behavior, due to which the agents are on average attracted to the center of the group while moving forward.

A similar slowing down and jamming has been found by Deneubourg et al. [7] in a model that closely resembles the swarming behavior of army ants. Further, exactly these school characteristics (of frontal density and oblong groups) have been found in shoals of roach (*Rutilus rutilus*) by Bumann et al. [4]. Using models of predation minimization and corresponding experimental procedures on creek chub (*Semotilus actromaculatus*), the authors conclude that both increased density in the front of the school and elongated shape of groups are ways to minimize the predation risk by hiding from the periphery and behind others (as suggested by the selfish-herd theory; see [8]). Bumann et al., however, do not offer any ideas how individual fish may attain such characteristics of school form and heterogeneous density. SchoolingWorld suggests a solution: An oblong group shape and the highest density at the front of the school may automatically result from the simple behavioral rules of repulsion, alignment, and attraction.

Note that even though we provided agents with a speed that is fixed with random noise (as is also done in the other models [1, 6, 10]), the front agents still appear to be slowing down, and the effects on group structure and size closely resemble patterns that have been studied in fish. This minimal representation, thus, seems to suffice to reproduce these phenomena. On the other hand, adaptation of speed between neighboring agents would be an interesting extension to study in future models.

As regards our preliminary representation of embodiment, we have compared the effect of two body sizes and of three body forms (point, line, and ellipse) on patterns of schooling for a range of different school sizes. As regards size of the agent, larger body size is accompanied by a larger area of repulsion and alignment, and therefore the nearest neighbor distance is larger and coordination is stronger among large than among small (point and line, but not elliptical) agents. These results are in agreement with those by Olst and Hunter [14] in their comparative study between adult and juvenile (instead of large and small) fish. Olst and Hunter, however, attribute the lower cohesion and alignment to the higher feeding rates of juvenile fish, whereas in our model these differences are a direct consequence of body size, that is, size of the region of repulsion and alignment.

Of the three body forms, groups of line agents have, compared to those of point agents, a slightly larger average center distance, and they are wider, longer, and less homogeneous; their other school characteristics are similar. The greatest differences are found between elliptical agents and the others. Groups of elliptical agents are more cohesive (in average center distance as well as nearest neighbor distance); they are less homogeneous, because the inter-individual distance of agents swimming side by side is much shorter than those swimming in file. Further, they show higher confusion, and confusion is greater among large agents than small ones, whereas among point and line

agents the reverse holds. These phenomena are directly related to the elliptical form of the repulsion region (which is more asymmetric for the large agents), which in turn is associated with the repeated repulsion effect. Although intuitively the representation of a fish as an elliptical agent seems more natural than as a point or line agent, this cannot be judged at present from the results. In this context, it is of interest to compare confusion among groups of small adult individuals and large ones of the same species: if confusion is greater among the larger individuals, this will provide support for the model of elliptical agents as being a better representation than that of point and line agents.

This is, of course, still a preliminary representation of the body, and each level of detail that will be added in future (such as a body that can bend) may lead to new hypotheses as regards collective phenomena in real fish. The main function of models like SchoolingWorld may be to provide us with useful new hypotheses.

Acknowledgments

We thank Jan Wantia and Jens Krause for helpful comments on an earlier version of the manuscript, and Rolf Pfeifer for continuous support. This work is partly financed by a grant from the A. H. Schultz foundation and from the Swiss National Science Foundation (31-065444) to Charlotte Hemelrijk.

References

1. Aoki, I. (1982). A simulation study on the schooling mechanism in fish. *Bulletin of the Japan Society of Scientific Fisheries, 48*, 1081–1088.
2. Bleckman, H. (1993). Role of the lateral line in fish behaviour. In T. Pitcher (Ed.), *Behaviour of teleost fishes*. London: Chapman and Hall.
3. Breeder, J. M. (1954). Equations descriptive of fish schools and other animal aggregations. *Ecology, 35*(3), 361–369.
4. Bumann, D., Krause, J., & Rubenstein, D. (1997). Mortality risk of spatial positions in animal groups: The danger of being in the front. *Behaviour, 134*, 1063–1076.
5. Camazine, S., Deneubourg, J. L., Franks, N. R., Sneyd, J., Theraulaz, G., & Bonabeau, E. (2001). *Self-organization in biological systems*. Princeton and Oxford: Princeton University Press.
6. Couzin, I. D., Krause, J., James, R., Ruxton, G. D., & Franks, N. R. (2002). Collective memory and spatial sorting in animal groups. *Journal of Theoretical Biology, 218*, 1–11.
7. Deneubourg, J. L., Goss, S., Franks, N., & Pasteels, J. M. (1989). The blind leading the blind: Modelling chemically mediated army ant raid patterns. *Journal of Insect Behaviour, 2*, 719–725.
8. Hamilton, W. D. (1971). Geometry for the selfish herd. *Journal of Theoretical Biology, 31*, 295–311.
9. Huth, A. (1992). *Ein Simulationsmodell zur Erklärung der Kooperativen Bewegung von polarisierten Fischschwärmen*. Marburg: Department of Biology and Physics, University of Marburg.
10. Huth, A., & Wissel, C. (1992). The simulation of the movement of fish schools. *Journal of Theoretical Biology, 156*, 365–385.
11. Huth, A., & Wissel, C. (1994). The analysis of behaviour and the structure of fish schools by means of computer simulations. *Comments in Theoretical Biology, 3*, 169–201.
12. Huth, A., & Wissel, C. (1994). The simulation of fish schools in comparison with experimental data. *Ecological Modelling, 75/76*, 135–145.
13. Niwa, H.-S. (1994). Self-organizing dynamic model of fish schooling. *Journal of Theoretical Biology, 171*, 123–136.

14. Olst, J. C. v., & Hunter, J. R. (1970). Some aspects of the organization of fish schools. *Journal of the Fisheries Research Board of Canada, 27*, 1225–1238.

15. Partridge, B. L. (1980). The effect of school size on the structure and dynamics of minnow schools. *Animal Behaviour, 28*, 68–77.

16. Partridge, B. L., Pitcher, T., Cullen, J. M., & Wilson, J. (1980). The three-dimensional structure of fish schools. *Behavioral Ecology and Sociobiology, 6*, 277–288.

17. Partridge, B. L., & Pitcher, T. J. (1980). The sensory basis of fish schools: Relative roles of lateral line and vision. *Journal of Comparative Physiology, 135*, 315–325.

18. Pfeifer, R., & Scheier, C. (1999). *Understanding intelligence*. Cambridge, MA: MIT Press.

19. Pfeifer, R. (2000). On the role of embodiment in the emergence of cognition and emotion. In G. Hatano, N. Okada, and H. Tanabe (Eds.), *Affective Minds: Proceedings of the 13th Toyota Conference, Shizuoka, Japan, 1999* (pp. 43–58). Elsevier Science.

20. Reuter, H., & Breckling, B. (1994). Self organisation of fish schools: An object-oriented model. *Ecological Modelling, 75/76*, 147–159.

21. Reynolds, C. W. (1987). Flocks, herds and schools: A distributed behavioral model. *Computer Graphics, 21*(4), 25–36.

22. Romey, W. L. (1996). Individual differences make a difference in the trajectories of simulated schools of fish. *Ecological Modelling, 92*(1), 65–77.

23. Shaw, E. (1970). Schooling in fishes: Critique and review. In L. Aronson (Ed.), *Development and Evolution of Behavior* (pp. 452–480). San Francisco: Freeman.

24. Vabo, R., & Nottestad, L. (1997). An individual based model of fish school reactions: Predicting antipredator behaviour as observed in nature. *Fisheries Oceanography, 6*(3), 155–171.

25. Warburton, K., & Lazarus, J. (1991). Tendency-distance models of social cohesion in animal groups. *Journal of Theoretical Biology, 150*, 473–488.